FLOMEKO 2022

Study on the Uncertainty of the Doppler Frequency for the Calibration of LDV within the Speed of (0.1~340) m/s

Y. W. Zhang[1,2], L. S. Cui[2], D. L. Xie[1], H. Zhang[3]
[1]China Jiliang University, Xue Yuan Jie 258#, Hangzhou, Zhejiang, China
[2]National Institute of Metrology, Beijing, China
[3]Beijing Gas Group Company Limited, Beijing, China
E-mail (corresponding author): cuils@nim.ac.cn

Abstract

Laser Doppler Velocimetry (LDV) is a single-point velocity measurement instrument. LDV can be precisely calibrated by the adjustable speed spinning-dics facility from NIM at speeds generally less than 40 m/s. However, due to its unique limitations, it is hard to calibrate LDV at a higher speed. To solve the problem of traceability of LDV high-speed measurement results and of the applicability of LDV low-speed calibration results under high-speed conditions, it is analyzed that the uncertainty of velocity depends on both interference fringe spacing and Doppler frequency. As fringe spacing is independent of velocity, the possible difference of uncertainty in between the high and low velocity may be only related to the uncertainty of Doppler frequency at different velocities. Doppler frequency is a result of Doppler frequency algorithm, which includes mixed-radix FFT (Fast Fourier Transform) and the phase difference correction method in this paper. Because of the nonlinearity and complexity of the algorithm, the uncertainty of Doppler frequency is suitable for being evaluated by Monte Carlo Method (MCM) propagating probability distribution. The evaluation result shows that the relative uncertainty of Doppler frequency caused by the algorithm is less than 0.05% within the range of (0.1~340) m/s. The obvious difference of uncertainty has not been found in different velocities investigated. The budget resulting from Doppler frequency uncertainty change on the velocity result is less than 0.00075%. It is concluded that the calibration result at low velocity is also reasonable to be used in the case at the high velocity measurement within the speed of (0.1~340) m/s.

1. Introduction

Laser Doppler Velocimetry (LDV) is a single-point velocity measurement instrument which has high-precision and non-contact properties. It is suitable for the measurement of flow velocities within (0.1~340) m/s and widely used in fields such as deep diving exploration, military production and satellite navigation [1-3]. Velocity measured by LDV is related to the interference fringe spacing in the measurement volume and Doppler frequency [4] and their measurement uncertainties are also related correspondingly. Fringe spacing can be calibrated by the adjustable-speed spinning-disc facility below 40 m/s [5]. And the value of fringe spacing depends only on the wavelength of the Laser and the angle between two coherent beams so the uncertainty of the fringe spacing keeps unchanged at different velocities theoretically [4]. Additionally, Doppler frequency is calculated by the Doppler frequency algorithm, and it can be inferred that the change of velocity uncertainty at different velocities may be caused by that of the Doppler frequency uncertainty. Therefore, study on the changes of the Doppler frequency uncertainty caused by the algorithm at different velocities is aimed at evaluation and expression of the measurement results of LDV at high speed so as to solve the traceability problem of the high velocity measurement of LDV.

The uncertainty is often evaluated according to the *Guide to the Expression of Uncertainty in Measurement* (GUM) in the National Metrology Calibration Standard JJF 1059.1-2012 [6]. But GUM has certain limitations of application. In this paper, the Doppler frequency algorithm is composed of mixed-radix FFT and phase difference correction method. The model of the algorithm is nonlinear; it is difficult to display the explicit functions of some inputs; the distribution of output values keeps unknown. So it is impossible to accurately judge the applicability of the uncertainty which is caused by the algorithm evaluated by GUM. Hence the method of Monte Carlo Method (MCM) propagating probability distribution is proposed to evaluate the uncertainty of Doppler frequency caused by the algorithm. It is suitable for the conditions: the model is nonlinear; it is hard to calculate partial derivative of model; PDF of output values deviates from the normal or t-distribution [7].

2. Doppler frequency calculation model

The relationship between the velocity v and Doppler frequency f_D is linear [8]. Doppler frequency is chosen as the output during calculation which is as follows: the LDV signal processing system picks up the scattered light signal and converts that photoelectric signal to an analogue continuous signal. The signal $x(t)$ is cut off by a rectangular window function $w_N(t)$ with length N and

then it is sampled into a finite discrete signal for data processing by the data processing system, as shown in the Equation (1).

$$x^{(\mathrm{raw})}(t) = x(t)\,w_N(t),\ t \in [0,\ N-1] \tag{1}$$

After sampling the finite continuous signal $x^{(\mathrm{raw})}(t)$ with the sampling frequency f_s, the discrete sampling signal $x(n)$ is obtained in the Equation (2).

$$\begin{aligned} x(n) &= x^{(\mathrm{raw})}(t)\Big|_{t=\frac{n}{f_s}} \\ &= x^{(\mathrm{raw})}\left(\frac{n}{f_s}\right),\ n = 0,1,\ldots,\ N-1 \end{aligned} \tag{2}$$

Where $x(n)$ is a discrete signal of length N, which is used as the input to mixed-radix Fast Fourier Transform (FFT). And then the spectrum $X(k)$ of signal is calculated to solve for Doppler frequency. Mixed-radix FFT is an iterative algorithm that performs Discrete Fourier Transform (DFT) by factoring length N of signal into mixed radix, as shown in Equation (3).

$$N = r_1 r_2 \cdots r_L \tag{3}$$

Where r_1, r_2, …, r_L are the different prime factors; L is the total number of the primes. And the formula of mixed-radix FFT is shown in Equation (4) [9, 10].

$$\begin{aligned} X(k) &= \sum_{n=0}^{N-1}\left[x(n)W_N^{nk}\right] \\ &= \sum_{n_0=0}^{r_L-1}\sum_{n_1=0}^{r_{L-1}-1}\cdots\sum_{n_{L-1}=0}^{r_1-1}\left\{x(n_{L-1},n_{L-2},\ldots,n_0)W_N^{\left[k_0(r_1r_2\cdots r_{L-1})+k_1(r_1r_2\cdots r_{L-2})+\cdots+k_{L-2}(r_1)+k_{L-1}\right]\left[n_{L-1}(r_2r_3\cdots r_L)+n_{L-2}(r_3r_4\cdots r_L)+\cdots+n_1(r_L)+n_0\right]}\right\} \end{aligned} \tag{4}$$

Where W_N^{para}, W_N^{fac} are coefficient rotation factor and DFT rotation factor [9, 10]. $x(n)$ is substituted into Equation (4) to acquire the signal amplitude spectrum $|X(k)|$. According to the principle of Doppler frequency calculation and the relationship between frequency and its sequence number k, the number of the maximum value k_D of the amplitude spectrum can be obtained, which is used to calculate uncorrected Doppler frequency f_D' in the Equations (5) and (6).

$$k_D = g^{-1}\left(\max\left\{\left|X(k)\right|\right\}\right) \tag{5}$$

$$f_D' = k_D\frac{f_s}{N} \tag{6}$$

When performing asynchronous sampling or non-integer period truncation, spectral leakage and picket fence effect will occur, so Doppler frequency will deviate from its true value to a certain extent. Consequently it is necessary to correct the frequency sequence numbers by using phase difference correction method in spectrum. The correction is as shown in Equation (7) [11].

$$f_D = \frac{(k_D+\Delta k)}{k_D}f_D' = (k_D+\Delta k)\frac{f_s}{N} \tag{7}$$

Where Δk is the frequency sequence numbers correction; f_D is the corrected Doppler frequency (true value theoretically); g^{-1} is an inverse function.

And the component R_1 caused by rounding appears at the positions involving addition and multiplication operations. Since k_D is an integer, there isn't the rounding component. After Rewriting Equations (5), (6) and (7) with R_1, the complete calculation model of Doppler frequency is shown in Equation (8), where the components $R_1^{(j)}$ (j=1,2, …, 7) are the same type of components due to rounding, but may differ in value.

$$\begin{cases} \max\left\{\left|X(k)\right|\right\} \\ = \max\left\{\left|\sum_n\left\{\left[x(n)W_N^{(\mathrm{para})} - R_1^{(1)}\right]W_N^{(\mathrm{fac})} - R_1^{(2)}\right\} - R_1^{(3)}\right|\right\} \\ k_D = g^{-1}\left(\max\left\{\left|X(k)\right|\right\}\right) \\ f_D' = k_D\left(\frac{f_s}{N} - R_1^{(4)}\right) - R_1^{(5)} \\ f_D = \left(\frac{(k_D+\Delta k)}{k_D} - R_1^{(6)}\right)f_D' - R_1^{(7)} \end{cases} \tag{8}$$

3. Doppler frequency evaluation by the method of MCM propagating PDF

The steps of uncertainty evaluation by the method of MCM propagating PDF are mainly divided into four steps: MCM inputs, MCM propagation, MCM output and result representation [7], as follows:

Firstly, the inputs X_i, i = 1, 2, …, L, the output Y and the calculation model of them should be determined. Then PDFs are set for each input X_i respectively and MCM test sample size M is selected. M samples are chosen from their respective PDFs of X_i as the inputs, and M outputs Y are obtained through model calculation. Those M outputs are arranged in a strict increasing order to get the discrete PDF $\boldsymbol{G}$ of the output, from which the estimate $\bar{y}$ of Y, the standard deviation $\sigma(y)$ and the inclusion interval $[y_{\mathrm{Lower}}, y_{\mathrm{Upper}}]$ of Y under a given probability p can be expressed at last.

3.1 MCM inputs of Doppler frequency algorithm

According to the calculation model, the input sources of uncertainty caused by Doppler frequency algorithm are analyzed. The Doppler signal is composed of the Gaussian distributed base signal (low frequency) and the envelope of the Gaussian distributed cosine signal (high frequency) [4], as shown in Equation (9).

$$x(t)=x_1\exp\left[-\frac{\left(2\sqrt{2}t\right)^2}{\tau^2}\right]+x_2\exp\left[-\frac{\left(2\sqrt{2}t\right)^2}{\tau^2}\right]\cos\left(2\pi f_D t+\theta_0\right) \quad (9)$$

Where t is the time; $\tau=N_s/f_D$ is the finite transit time of the particle passing through the measurement volume; f_D is the true value of Doppler frequency; N_s represents the number of fringes in the measurement volume, which is related to the measuring volume diameter and the size of the fringe spacing; x_1, x_2 are the amplitude of the low and high frequency signal in Doppler signal respectively.

After high-pass filtering, according to the characteristics of the signal amplitude, Doppler signal can be expressed as a continuous constant amplitude wave (x_2 is time-invariant) or continuous random amplitude wave. And the former wave is selected for the evaluation (the evaluation method of the latter is the same), as shown in Equation (10) [4].

$$x(t)=x_2\exp\left[-\frac{\left(2\sqrt{2}tf_D\right)^2}{N_s^2}\right]\cos\left(2\pi f_D t+\theta_0\right) \quad (10)$$

Then the continuous signal $x(t)$ is cut off by a window function through Equation (1) and sampled through Equation (2) to become a discrete sequence $x(n)$, as shown in Equation (11).

$$x(n)=x_2\exp\left[-\frac{\left(2\sqrt{2}nf_D\right)^2}{N_s^2}\right]\cos\left(2\pi f_D n+\theta_0\right) \quad (11)$$

Where n=0, 1, …, N–1; θ_0 is the initial phase of the signal. From Equation (8), it is obtained that x_2、N_s is unrelated to Doppler frequency. Thus they are set as the constant x_2=1、N_s=21. f_D is also an unknown constant, so there is the only input θ_0 in Equation (9); In the calculation process of mixed-radix FFT, the output is only related to input $x(n)$, so there is the only input θ_0, too; The sources of inputs in Equation (6) are the sampling frequency f_s and the length N; The input in Equation (7) is the spectral correction Δk; Finally, there is the component R_1 introduced by rounding. And the calculation model is built and shown in Equation (12).

$$f_D=f\left(\theta_0,\ f_s,\ N,\ \Delta k,\ R_1\right) \quad (12)$$

3.2 Evaluation analysis of uncertainty introduced by rounding

In computer operations, real numbers are represented by rounding as the floating-point numbers [12]. And the uncertainty introduced by rounding will appear anywhere in the operations performed by the computer. Therefore, the degree and influence of the uncertainty introduced by rounding need be firstly analyzed in this section for the basis of analysis in subsequent chapters.

The data is generally expressed as an approximation of the original data by the regulation of the rounding principle. The rounding number can only be an integer multiple of the rounding interval δ and the maximum error introduced after rounding is $\delta/2$, which is uniform distributed [12, 13]. According to the B-type evaluation method of standard uncertainty, the interval half-width a can be expressed as the maximum error $\delta/2$ with confidence factor $k=\sqrt{3}$, and the uncertainty introduced by rounding is shown in Equation (13).

$$u_\delta(x)=\frac{a}{k}=\frac{\delta}{2\sqrt{3}}=0.29\delta \quad (13)$$

In the operation process, there is rounding in both multiplication and addition. The rounding uncertainty introduced by one round of multiplication is shown in Equation (14).

$$u_\delta^{\text{mul}}=\frac{a}{k}=\frac{\delta}{2\sqrt{3}}=0.29\delta \quad (14)$$

The rounding uncertainty introduced by one round of addition is shown in Equation (15).

$$u_\delta^{\text{add}}=\frac{a}{k}=\frac{\delta}{2\sqrt{3}}=0.29\delta \quad (15)$$

In the process of mixed-radix FFT, DFT is divided into L layers for iterative operation. And each layer is composed of the sum of product of the input sequence, the coefficient rotation factor and the DFT rotation factor. Therefore, the operation of each layer contains the multiplication of three complex numbers and then in turn add up. The multiplication containing 3 complex numbers requires 8 real number multiplication and 3 real number addition operations. Similarly, there are 8 imaginary number multiplication and 3 imaginary number addition operations. After complex multiplication, r_m–1 (r_m is the size of items in m^{th} layer) complex addition are required, so the real part rounding uncertainty of the m^{th} layer of output are shown in Equation (16).

$$\begin{aligned}e_{R,m}&=8\times u_\delta^{\text{mul}}+\left(3+r_m-1\right)\times u_\delta^{\text{add}}\\&=\left(10+r_m\right)\times 0.29\delta\end{aligned} \quad (16)$$

The imaginary part is shown in Equation (17).

$$\begin{aligned}e_{I,m}&=8\times u_\delta^{\text{mul}}+\left(3+r_m-1\right)\times u_\delta^{\text{add}}\\&=\left(10+r_m\right)\times 0.29\delta\end{aligned} \quad (17)$$

The total amplitude rounding uncertainty of the m^{th} layer is shown in Equation (18).

$$e_{A,m}=\sqrt{e_{R,m}^2+e_{I,m}^2}=\sqrt{2}e_{R,m} \quad (18)$$

In the mixed-radix FFT calculation process, the amplitude uncertainty generated by each layer will be transferred to the next layer in the form of addition. The total amplitude rounding uncertainty in the L^{th} layer is shown in Equation (19):

$$e_m = \sum_{m=1}^{L} e_{A,m} = \sum_{m=1}^{L} \sqrt{2} e_{R,m} \tag{19}$$

Assuming that the number of reserved digits is q. So the rounding interval is $\delta = 1\times10^{-q}$ and the half-width of the interval $a = \delta/2 = 0.5\times10^{-q}$. There are different points of signal analysis in Table 1. where N is the number of discrete signal points (same as windowing length), and $sum()$ represents the summation function.

Table 1: Relationship between different reserved digits and rounding uncertainty of different points

$(N, L, sum(r_m))(r_m)$ $(m=1, 2, \ldots, L)$	Rounding Uncertainty			
	8 bits	**16 bits**	**32 bits**	**64 bits**
(30, 3, 10) (2, 3, 5)	1.64e-7	1.64e-15	1.64e-31	1.64e-63
(210, 4, 17) (2, 3, 5, 7)	2.34e-7	2.34e-15	2.34e-31	2.34e-63
(2310, 5, 28) (2, 3, 5, 7, 11)	3.20e-7	3.20e-15	3.20e-31	3.20e-63
(30030, 6, 41) (2, 3, 5, 7, 11, 13)	4.14e-7	4.14e-15	4.14e-31	4.14e-63
(128, 7, 14) (2, 2, 2, 2, 2, 2, 2)	3.46e-7	3.46e-15	3.46e-31	3.46e-63

From Table 1, it is obtained that the uncertainty introduced by rounding can be ignored in the condition that the number of reserved significant digits are 4 or less. In the MATLAB environment, the number of reserved digits can be 15 in general and in the process of Doppler frequency calculation the order of magnitudes of Doppler frequency is tens of millions or less, so the number of reserved digits are 7 or more. The number of reversed digits in this evaluation are all 4, so the influence of the uncertainty introduced by rounding can be ignored.

3.3 Probability distribution of inputs

Based on the characteristics of different inputs in Equation (12), PDFs are set for them.

When the continuous signal is cut off by window function, the probability of the origin of the signal depends on its initial phase θ_0 which is uniform distribution, $\theta_0 \sim R(-\pi,\pi)$.

LDV can be applied in (0.1~340) m/s velocity measurement in practice and the corresponding range of Doppler frequency is around (10, 000~50, 000, 000) Hz. The sampling frequency f_s which is set artificially need satisfy the sampling theorem and should not be too large. So the sampling frequency f_s is chosen as uniform distribution, $f_s \sim R(2.56f_D, 3f_D)$. Similarly, for efficiency the length N should be set as large as possible but not too large. The length N is set as an integer between 128 and 16384, $N \sim R(128,16384)$.

The rounding component R_1 has a same probability of appearing everywhere within the error limitation, which satisfies the uniform distribution [13, 14].

In the process of spectrum correction, spectral correction Δk is related to initial phase, sampling frequency f_s and length N, which are all uniform distribution [11].

To sum up, each input can be set as uniform distribution, and its range is shown in Table 2. Where (a, b) is the range of each input.

Table 2: The range of inputs

Inputs	**Sources**	***a***	***b***	**Note**
θ_0	Initial Phase	$-\pi$	π	
f_s	Sampling Frequency	$2.56f_D$	$3f_D$	(0.1~340) m/s
N	Length	128	16384	Efficiency
R_1	Rounding	$-\delta/2$	$\delta/2$	δ depends on reserved digits
Δk	phase difference correction method			Related to other inputs

3.4 MCM propagation, output and result representation of mixed-radix FFT

Inclusion probability p is set to 95% and the test sample size M needs satisfy $M \geq 1/(1-p)\times10^4 = 200000$ [7]. So the comparison between $M=2\times10^5$ and $M=10^6$ is made at the same time for accuracy and efficiency. The process of propagation is as follows: the test sample size is set to M; The input vector $(\theta_0, f_s, N, \Delta k, R_1)$ is randomly sampled M times and output $(f_{D1}, f_{D2}, \ldots, f_{DM})$ is obtained; Then the output values are arranged into vectors in a strict increasing order from smallest to largest $(f_{D(1)}, f_{D(2)}, \ldots, f_{D(M)})$($f_{D(1)} \leq f_{D(2)} \leq \ldots \leq f_{D(M)}$), from which the discrete probability density function $\boldsymbol{G}$ is calculated. Finally, the estimate $\overline{f}_D$, the standard deviation $\sigma(f_D)$ and inclusion interval $[f_{D-Lower}, f_{D-Upper}]$ with probability p=95% are expressed from the vectors $(f_{D1}, f_{D2}, \ldots, f_{DM})$ in $\boldsymbol{G}(f_D)$. The theoretical Doppler frequencies at different flow velocities are calculated respectively under the conditions that the laser wavelength is 514.5 nm, the angle between the laser beams is 0.0379 rad, the beam diameter is 2.2 mm, and the spacing between the two laser beams is 37.91 mm. Then the simulation signal $x(n)$ as shown in Equation (11) is generated for evaluation in MATLAB. And the average of three evaluations of the estimate $\overline{f}_D$, the standard deviation $\sigma(f_D)$ and inclusion interval $[f_{D-Lower}, f_{D-Upper}]$ with probability p=95% are taken as the final MCM evaluation results. The results of the evaluation and Doppler frequency under $M=2\times10^5$ and $M=10^6$ are as shown in Table 3 and 4 respectively.

Table 3: MCM results of Doppler frequency (M =2×10^5).

Velocity (m/s)	Theoretical Doppler frequency (Hz)	M =2×10^5		
		$\overline{f}_D$/Hz	σ(f_D)/Hz	[$f_{D-Lower}$, $f_{D-Upper}$] /Hz (p = 95%)
0.1	14724	14723.9991	5.9544	[14716.8633, 14730.9942]
0.5	73626	73625.8290	29.5184	[73590.0051, 73660.8646]
1	147252	147251.9764	59.4845	[147180.6818, 147321.7592]
5	736267	736266.5152	296.9699	[735909.7353, 736617.5596]
10	1472532	1472531.0076	593.9419	[1471817.2322, 1473232.8709]
15	2208802	2208801.4068	894.0229	[2207732.4541, 2209851.8038]
20	2945067	2945064.4867	1183.9721	[2943651.5049, 2946476.0923]
50	7362669	7362662.0759	2942.9942	[7359123.7751, 7366183.3443]
100	14725338	14725329.5135	5941.7293	[14718186.1030, 14732330.1185]
200	29450676	29450658.9674	11883.3832	[29436372.0059, 29464654.5805]
300	44176017	44175975.5577	17645.6656	[44154787.0402, 44197094.6815]
340	50066153	50066061.8656	20078.5820	[50041546.3603, 50089604.5680]

Table 4: MCM results of Doppler frequency (M =10^6).

Velocity (m/s)	Theoretical Doppler frequency (Hz)	M =10^6		
		$\overline{f}_D$/Hz	σ(f_D)/Hz	[$f_{D-Lower}$, $f_{D-Upper}$] /Hz (p = 95%)
0.1	14724	14723.9837	5.8974	[14716.8575, 14730.9654]
0.5	73626	73625.9553	29.5407	[73590.4846, 73660.9661]
1	147252	147251.8369	59.0319	[147180.4730, 147321.6641]
5	736267	736266.2137	295.0303	[735909.4439, 736615.1437]
10	1472532	1472530.4225	590.0636	[1471816.9244, 1473228.2730]
15	2208802	2208799.5178	885.0677	[2207729.0882, 2209846.6842]
20	2945067	2945064.3674	1182.2896	[2943638.9532, 2946467.5529]
50	7362669	7362660.8335	2952.2199	[7359094.7329, 7366152.5426]
100	14725338	14725323.1111	5913.8107	[14718190.9383, 14732342.8105]
200	29450676	29450649.7897	11814.9338	[29436411.7298, 29464709.7279]
300	44176017	44175977.6602	17722.4010	[44154620.7114, 44197067.7329]
340	50066153	50066104.0691	20105.6080	[50041857.3353, 50089963.9321]

4. Results analysis

Based on the Table 3 and 4, it is analyzed that the evaluation results of MCM with M =2×10^5 and M =10^6 are compared with inclusion probability p=95%. The results are composed of the estimate $\overline{f}_D$, the interval length | $f_{D-Upper}$− $f_{D-Lower}$| and their relative value respectively, as shown in Table 5 and 6.

Table 5: The estimate relative value under different test sample size

Velocity (m/s)	The estimate $\overline{f}_D$		
	M =2×10^5	M =10^6	Relative value
0.1	14723.9991	14723.9837	1.05×10^{-6}
0.5	73625.8290	73625.9553	1.72×10^{-6}
1	147251.9764	147251.8369	9.47×10^{-7}
5	736266.5152	736266.2137	4.10×10^{-7}
10	1472531.0076	1472530.4225	3.97×10^{-7}
15	2208801.4068	2208799.5178	8.55×10^{-7}
20	2945064.4867	2945064.3674	4.05×10^{-8}
50	7362662.0759	7362660.8335	1.69×10^{-7}
100	14725329.5135	14725323.1111	4.35×10^{-7}
200	29450658.9674	29450649.7897	3.12×10^{-7}
300	44175975.5577	44175977.6602	4.76×10^{-8}
340	50066061.8656	50066104.0691	8.43×10^{-7}

Table 6: Interval length relative value under different test sample size

Velocity (m/s)	Interval length	$f_{D-Upper}$− $f_{D-Lower}$|	
	M =2×10^5	M =10^6	Relative value
0.1	14.1309	14.1079	1.63×10^{-3}
0.5	70.8595	70.4815	5.36×10^{-3}
1	141.0774	141.1911	8.05×10^{-4}
5	707.8243	705.6998	3.01×10^{-3}
10	1415.6387	1411.3486	3.04×10^{-3}
15	2119.3497	2117.596	8.28×10^{-4}
20	2824.5874	2828.5997	1.42×10^{-3}
50	7059.5692	7057.8097	2.49×10^{-4}
100	14144.0155	14151.8722	5.55×10^{-4}
200	28282.5746	28297.9981	5.45×10^{-4}
300	42307.6413	42447.0215	3.28×10^{-3}
340	48058.2077	48106.5968	1.01×10^{-3}

Firstly, from Table 5 and 6 that the relative value of the estimate is below the order of magnitude of 10^{-5}, and that of the corresponding interval length is below the order of magnitude of 10^{-2}. So there is little difference in the evaluation results between under the sample size of M =2×10^5 and M =10^6. Secondly, there are certain rules in the PDF of the Doppler frequency under different velocities. It is acquired that under different velocities the PDF of Doppler frequency after the evaluation shows a trend that tends to be the same distribution that the peaks are prominent in the middle; the peaks are sharply decreasing on both sides; the edges are flat on both sides. And the probability density values of the peaks, the interval length display a gradual decrease and a gradual increase trend respectively with the increasing velocity, as shown in Figure 1.

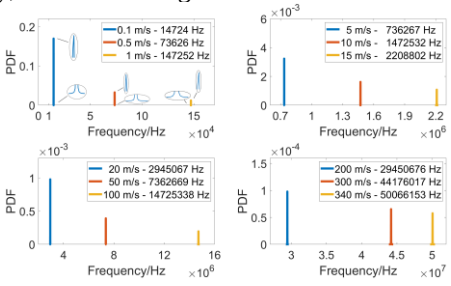

Figure 1: Doppler frequency PDF at different flow velocities

The corresponding uncertainty $u(f_D)$ is calculated based on the standard deviation $\sigma(f_D)$ from Table 5 and 6. It is observed that uncertainty $u(f_D)$ is increasing linearly with the increase of velocity. And the uncertainty $u(f_D)$ is divided by theoretical Doppler frequency to obtain the relative uncertainty of Doppler frequency $u_r(f_D)$, as shown in Table 7.

Table 7: Velocity and Doppler frequency relative uncertainty

Velocity (m/s)	$u_r(f_D)$ (M =2×10^5)/%	$u_r(f_D)$ (M =10^6) /%
0.1	0.0404	0.0401 (min)
0.5	0.0401	0.0401
1	0.0401	0.0401
5	0.0403	0.0401
10	0.0403	0.0401
15	0.0405 (max)	0.0401
20	0.0402	0.0401
50	0.0400	0.0401
100	0.0404	0.0402 (max)
200	0.0404	0.0401
300	0.0399 (min)	0.0401
340	0.0401	0.0402

And it can be seen from Table 7 that the relative uncertainty of the Doppler frequency caused by the algorithm at different velocities is less than 0.05%. The maximum relative deviation between maximum and minimum of the relative uncertainty of Doppler frequency is 1.5%. And the budget of the change of the Doppler frequency measurement uncertainty at different velocities on the velocity measurement results was less than 0.00075%, which verified the applicable accuracy range of the Doppler frequency algorithm. Therefore, the LDV calibration results at low velocity can be reasonably applied at high velocity measurement and the traceability problem of the high velocity measurement of LDV has been solved.

5. Conclusion

(1) The influence of the uncertainty introduced by rounding on the uncertainty evaluation and the data processing process can be ignored in the condition that the number of reversed digits are less than 4.
(2) The effective results can be obtained under the test sample size is M=2×10^5 with inclusion probability p=95%.
(3) As the flow velocity increases, the uncertainty of Doppler frequency increases, but the relative uncertainty of Doppler frequency remains unchanged.
(4) The PDFs of Doppler frequency output values at different velocities tend to have the same distribution. And with the increase of velocity, the probability density values of the peaks, the interval length display a gradual decrease and a gradual increase trend respectively.
(5) The relative uncertainty of the Doppler frequency introduced by the Doppler frequency algorithm is less than 0.05% within the velocity range of (0.1~340) m/s
(6) The budget of the change of the Doppler frequency measurement uncertainty at different velocities on the LDV velocity measurement results was less than 0.00075%, so the LDV low velocity calibration results can be applied to the measurement of high flow velocity, which solves the traceability of the LDV measurement results in the high velocity measurement.

References

[1] Shen Y, Preliminary Research on Laser Doppler Flow Velocity Measurement (Changsha, National University of Defense Technology), 2019.
[2] Ying Z H, Gao C F, Wang Q, et al, Application of High-Accuracy Laser Doppler Velocimeter in Self-Contained Land Navigation System, Chinese Journal of Lasers, 44(12), 153-160, 2017.
[3] Zhang J J, Zhang L, Zhen S L, et al, Deep-sea in-situ Laser Doppler velocity measurement system, Chinese Journal of Physics, 70(21), 150-156, 2021.
[4] Shen X, Technology and Application of Laser Doppler Velocimetry (Beijing, Tsinghua University publishing house co., ltd), 2004.
[5] Liu Z J, Research on the Calibration Method of Laser Doppler Velocimeter Based on Adjustable Speed Spinning-Disc Facility (Hangzhou, China Jiliang University), 2018.
[6] JJF 1059.1-2012: Evaluation and Expression of Uncertainty in Measurement, 2012.
[7] JJF 1059.2-2012: Monte Carlo Method for Evaluation of Measurement Uncertainty, 2012.
[8] Rudd M J, A new theoretical model for the laser Dopplermeter, Journal of Physics E: Scientific Instruments, 2(1), 55-58, 1969.
[9] Zhang Y W, Research on LDV Doppler Frequency Algorithm based on Mixed-Radix FFT and its Introduced Uncertainty Evaluation (Hangzhou, China Jiliang University), 2022.
[10] Cheng P Q, Digital Signal Processing Tutorial (Beijing, Tsinghua University publishing house co., ltd), 2007.
[11] Xie M, Zhang X F, Ding K, A Phase Difference Correction Method for Phase and Frequency Correction in Spectral Analysis, Journal of Vibration Engineering, 12 (04), 18-23, 1999.
[12] Jing X D, Chen Z, Zhang Z H, et al, The Round-off Uncertainty Evaluation of Fast Fourier Transform, Acta Metrologica Sinica, 37(01), 105-108, 2016.
[13] Ni Y C, Practical Measurement Uncertainty Evaluation (Beijing, China Metrology Press), 2009.
[14] Li S A, JJF 1059-1999 Evaluation and Expression of Uncertainty in Measurement Discussion 37, Uncertainty Caused by Numerical Rounding, 21(06), 34-35, 2011.
[15] Jing X D, Chen Z, Ding H, Truncation Uncertainty Evaluation of Fast Fourier Transform Algorithm, Ship Engineering, 38(07): 67-69, 2016.